

Role of Ferrel cell in daily variability of Northern Hemisphere Annular Mode

Xiao-Feng Li · Jianping Li ·
Xiangdong Zhang · Cheng Sun

Received: 12 February 2014 / Accepted: 4 May 2014
© Science China Press and Springer-Verlag Berlin Heidelberg 2014

Abstract The Northern Hemisphere Annular Mode (NAM) represents the zonally symmetric planetary-scale atmospheric mass fluctuations between middle and high latitudes, whose variations have shown a large impact on other components of the climate system. Previous studies have indicated that the NAM is correlated with the Ferrel cell in their monthly or longer timescale variability. However, there have been few studies investigating their connections at daily timescale, though daily variability of NAM has been suggested to be an important component and has significant implication for weather forecast. The results from this study demonstrate that variability of the Ferrel cell leads that of the NAM by about 1–2 days. This statistically identified temporal phase difference between NAM and Ferrel cell variability can be elucidated by meridional mass redistribution. Intensified (weakened) Ferrel cell causes anomalously smaller (larger) poleward mass transport from the middle to the high latitudes, resulting in an increase (a decrease) in mass in the middle latitudes and a decrease (an increase) in the high latitudes. As a consequence, anomalously higher (lower) poleward pressure gradient forms and the NAM subsequently shifts to a positive (negative) phase at a time lag of 1–2 days. The findings here would augment the existing knowledge for better understanding the connection between the Ferrel

Cell and the NAM, and may provide skillful information for improving NAM as well as daily scale weather prediction.

Keywords Northern Hemisphere Annular Mode · Ferrel cell · Zonal mean circulations · Mass transportation · Surface pressure tendency · Prediction · Daily variability

1 Introduction

The Northern Hemisphere Annular Mode (NAM) is defined as the leading empirical orthogonal function (EOF) mode of the extratropical wintertime monthly sea level pressure (SLP) anomalies in the Northern Hemisphere (NH) [1, 2]. The NAM is characterized by its zonal symmetry, and represents the atmospheric mass difference between middle and high latitudes, and is essentially an internal atmospheric process that can be generated without external forcing [3, 4]. Due to these intrinsic properties, the NAM is usually treated as an important planetary-scale external factor that heavily influences the local climate [5–8] and other components of the climate system, such as ocean currents [9], sea ice [10], and terrestrial ecosystems [11].

To better understand NAM variability in zonally averaged circulations, the connections between the NAM and Ferrel cell have been studied over monthly and longer timescales. Thompson and Wallace [2] suggested that variation of the NAM is simultaneously correlated with that of the Ferrel cell and the poleward branch of the Hadley cell in month-to-month variability. Then Li and Wang [12] detected the Ferrel cell variability in the context of seasonal NAM fluctuations, and proposed that the

X.-F. Li · J. Li (✉) · C. Sun
State Key Laboratory of Numerical Modeling for Atmospheric Sciences and Geophysical Fluid Dynamics, Institute of Atmospheric Physics, Chinese Academy of Sciences, Beijing 100029, China
e-mail: ljp@lasg.iap.ac.cn

X. Zhang
International Arctic Research Center, University of Alaska Fairbanks, Fairbanks, Alaska 99775, USA

anomalous Ferrel cell is the primary meridional circulation bridging the two action centers of the NAM in zonally averaged circulations. This means that the NAM is closely connected with the Ferrel cell. However, few studies have focused on their connections at daily timescale, even though these daily timescale of around 10 days are known to be the intrinsic timescale of the NAM [13–15] and the daily variability of NAM has significant implication for weather forecast. Consequently, further study of the connections between the NAM and the Ferrel cell over short timescales is required, as this will help to improve our understanding of their internal linking processes, such as the role played by the Ferrel cell in the lifecycle of the NAM, etc. Furthermore, most studies focus on the momentum transport processes of the NAM [4, 16, 17], but few have considered mass transport processes related to the NAM, so the study of mass transportation processes offers a new perspective from which to develop our understanding of NAM variability. As the intensity of the Ferrel cell and NAM represent meridional mass transport, and mass distribution between middle and high latitudes, respectively, the study of links between the Ferrel cell and the NAM over short timescales will improve our understanding of mass transport and conservation processes within the life cycle of the NAM. Motivated by these factors, we re-investigate the connections between the NAM and the Ferrel cell, paying special attention to the role of the Ferrel cell in daily variability of the NAM and the related atmospheric mass transport processes.

2 Data and methodology

The daily and monthly data used in this study were the NCEP-NCAR reanalysis for 1958–2010 [18]. We focused on the winter season (November–December–January–February–March, NDJFM), which is the NAM's active season [2, 19]. The daily and monthly anomalies were obtained by subtracting their long-term climatological annual cycle calculated for the period 1958–2000. The NAM index (NAMI) proposed by Li and Wang [12] was used in this study, and is simply the normalized zonal mean difference in SLP between 35° and 65°N [20]. This NAMI performs well in capturing the NAM patterns and in capturing the relevant Ferrel cell variability. It should be noted that the main results of this study are not dependent on the choice of index, and that similar results are obtained when using the traditional NAMI defined using the EOF analysis from NOAA (<ftp://ftp.cpc.ncep.noaa.gov/cwlinks/>).

The Hadley cell index (HCI), Ferrel cell index (FCI), and Polar cell index (PCI) were used to represent the

intensity of the three meridional cells in the NH, and are defined as the maximum zonal mean meridional stream function (ZMSF) in the tropics (0°–30°N) [21–23], the minimum ZMSF in the middle latitudes (30°–60°N), and the maximum ZMSF in the polar regions (60°–90°N), respectively. The ZMSF, used to estimate the zonal mean meridional mass overturning circulation [21–23], is defined as

$$\text{ZMSF}(p, \varphi) = \frac{2\pi a \cos(\varphi)}{g} \int_P^{P_s} [v(p, \varphi)] dp, \quad (1)$$

where $[v]$ is the zonally averaged meridional wind, P is pressure, φ is latitude, g is the Earth's gravity, a is the Earth's radius, and P_s is surface pressure. As the ZMSF is negative in middle latitudes (30°–60°N), the final value of FCI is defined as a reversal of the minimum ZMSF in the middle latitudes, such that an intensified Ferrel cell is denoted by a larger value of the FCI.

Following the method proposed by Benedict et al. [24], a series of 21-day-span positive- and negative-phase NAM and Ferrel cell events were selected for composite analysis. A positive (negative) NAM or Ferrel cell event covers a 21-consecutive-day period, and contains at least 2 consecutive days when the NAMI or FCI is greater (less) than 1.5 standard deviations. The period of the NAM or FCI event is centered on the day with the highest (lowest) NAMI or FCI. The center day is labeled as the zero day, and hereafter labeled as the zero-lag day. The NAMI and FCI events were all selected in winters (NDJFM) between 1958 and 2009 due to their activity in this season, but were discarded if they extended into non-NDJFM months. Overall, the final selection used in this study comprised 93 positive and 81 negative NAMI events, and 89 positive and 78 negative FCI events.

3 General statistical relationship between the NAM and Ferrel cell

To understand the general co-variability between the NAM and the three meridional cells (Ferrel, Hadley, and Polar) in the NH, we conducted an initial statistical analysis based on the winter-to-winter fluctuations. The dominant feature was that the significant negative correlations between the NAM and ZMSF occur in the middle latitudes from 40° to 65°N (Fig. 1a). Relatively weak positive and negative correlations occur in the subtropics at approximately 10°–30°N, and in the polar region at 70°–85°N, respectively. A comparison with the wintertime climatologic distribution of the three cells (Fig. 1b) reveals that the largest correlation corresponds to the geographic location of the Ferrel cell, although with a

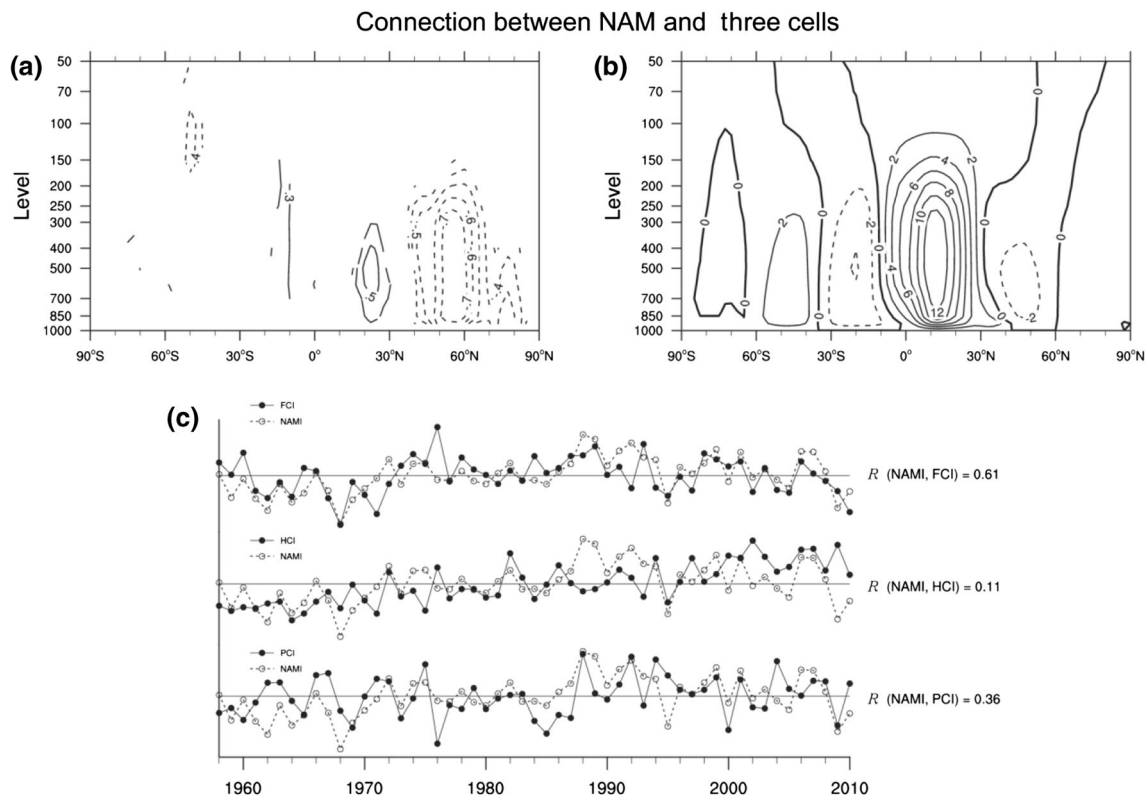


Fig. 1 **a** Map of correlation between the global zonal mean meridional stream function (ZMSF) in the winter (NDJFM) and NAMI for the period 1958–2010. Values above the 95 % confidence level are contoured (0.1 per contour interval); **b** Climatological global ZMSF for the same time period (unit: $10^{10} \text{ kg s}^{-1}$; heavy lines denote zero); **c** Three time series: normalized wintertime (DJF) NAMI with (top) the Ferrel cell index (FCI), (middle) the Hadley cell index (HCI), and (bottom) the Polar cell index (PCI). The correlation (R) between each pair of lines is presented at the end of the series and all exceed the 95 % confidence level

slight poleward shift. This suggests a tighter connection between the NAM and the Ferrel cell than that between the NAM and the Hadley or Polar cells, which is in good agreement with previous studies [2, 12].

We made a further comparison between the NAM and the three cells by examining their long-term time series (Fig. 1c), and confirmed that the Ferrel cell is connected most closely with the NAM. The temporal correlation coefficient between NAMI and FCI reaches 0.61, which is much higher than that between NAMI and either HCI (0.11) or PCI (0.36), suggesting that the Ferrel cell has the most synchronous variation with the NAM.

The remarkable similarity between the Ferrel cell and NAM variability can also be verified through their responses to changes in surface pressure (Fig. 2). The correlation coefficient between NAMI or FCI and wintertime surface pressure was calculated at each latitude [25]. Both the FCI and the NAMI have high negative values in the middle and high latitudes north of approximately 50° – 55°N , and have high positive values in the middle and low latitudes south of 50° – 55°N , indicating that both FCI and NAMI are associated with the mass diverging at middle

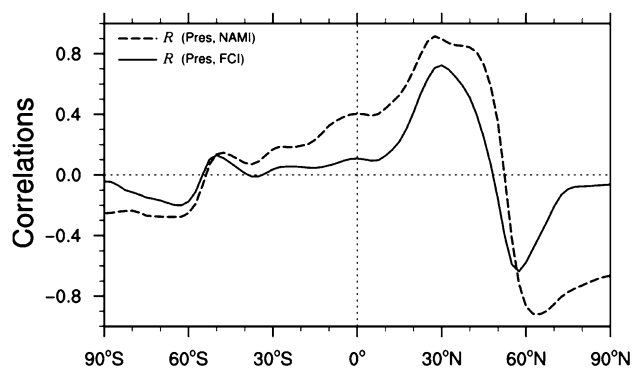


Fig. 2 Correlations between winter (NDJFM) surface pressure anomalies and the FCI (solid line) and NAMI (dashed line) for 1958–2010

and high latitudes, and the mass converging at middle and low latitudes. The meridional correlation coefficient between the NAMI and FCI curves in Fig. 2 reaches 0.87. This close correspondence indicates that the atmospheric mass distribution has very similar responses to the variations of the Ferrel cell and the NAM.

4 Daily fluctuations of the Ferrel cell precede those in the NAM

Although the high correlation between the Ferrel cell and the NAM in monthly and seasonal fluctuations has been observed in previous studies [2, 12], this does not mean that the Ferrel cell is varying synchronously with the NAM over daily timescales.

The lead-lag correlation between the FCI and the NAMI in daily data from the past 53 winters is shown in Fig. 3a. The significant positive lead-lag correlation between them reaches a maximum when the FCI precedes the NAMI by 1–2 days, and drops at the zero-lag day. This suggests that the variation of the NAM responds to the variation of the Ferrel cell about 1–2 days later, or the variation of the Ferrel cell precedes that of the NAM by about 1–2 days.

Figure 3b also shows that the variation of the Ferrel cell precedes that of the NAM. The value on each calendar day (365 days) is the lead-lag correlation coefficient between FCI and NAMI over the past 53 years, and a significant positive correlation occurs on most calendar days. Typically, the significant values first appear when FCI leads NAMI by about one week, attain a maximum when FCI

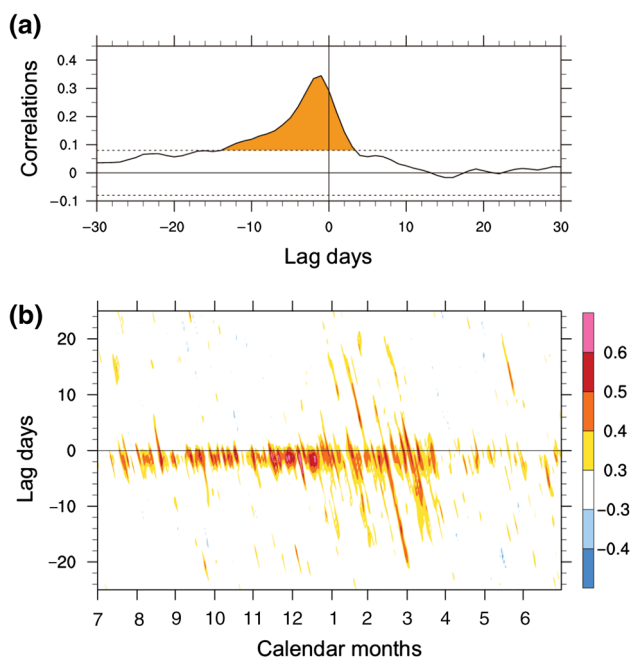


Fig. 3 Lag correlations between the FCI and the NAMI **a** for all winter days and **b** on the 365 calendar days (or 12 calendar months) of the 53 years between 1958 and 2010. Values above the 95 % confidence level are shaded in both panels. The effective degrees of freedom are estimated [40] in the top panel, considering its large sample number (6,360 days). Negative (positive) lag days denote FCI leading (lagging) NAMI. The FCI leads NAMI, in both cases, by at least one day

leads NAMI by about 1–2 days, then drops at the 0-lag day, as in Fig. 3a. Specifically, the significant lead-lag correlations during winter and early spring (DJFM) days first occur at an interval of more than two weeks, which is much earlier than that for the other seasonal calendar days. In addition, the lead-lag correlation values during late autumn and early winter (ND) are much stronger than those during other seasons. Therefore, the situation in which variation of the Ferrel cell precedes the NAM is a common phenomenon all year round, and this lead-lag relationship is especially strong in the active season of the NAM (NDJFM).

Time series of FCI and NAMI in observations during two sample time periods (Fig. 4) are also shown as examples to verify the above statistical lag relationship. During the period between 1 and 16 December 1984 (Fig. 4a), the variations of NAMI and FCI show both positive and negative phases. Over the whole period, the variation of FCI precedes NAMI by about one day. Similarly, this FCI-preceding-NAMI relationship also occurs during the period 4–21 December 1987, except that the preceding time at the beginning of the episode is about two days instead of one day. Thus, the lag relationship between the variation of the NAM and the Ferrel cell can be considered to be reliable, as it has been demonstrated to exist in real-time daily weather data.

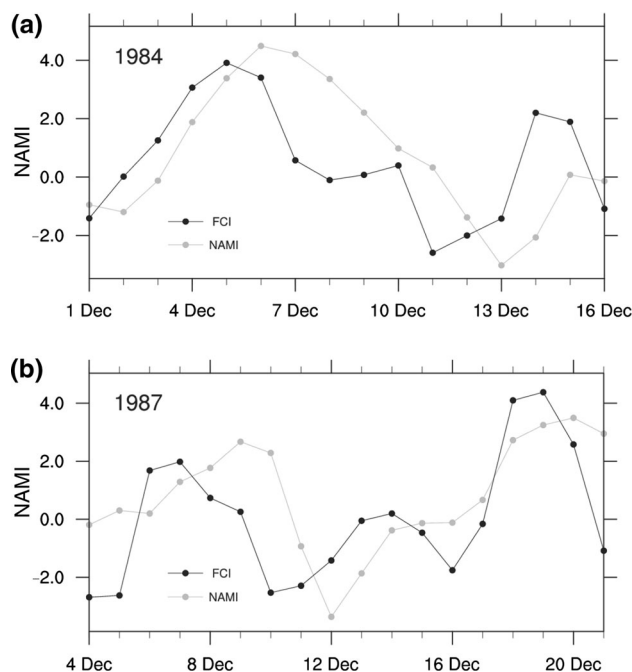


Fig. 4 Time series of FCI and NAMI during the periods **a** 1–16 December 1984, and **b** 4–21 December 1987

5 Theoretical analysis of the lag relationship between the Ferrel cell and the NAM over short timescales

To verify the existence of a statistical lag relationship between the Ferrel cell and the NAM, a theoretical analysis based on the surface pressure tendency equation [26] was also conducted. The left and right sides of the zonally averaged surface pressure tendency equation (Eq. (2)) represent the variation of the NAM and the Ferrel cell, respectively:

$$\frac{\partial C}{\partial t} \approx B, \quad (2)$$

$$C = [P_s], \quad (3)$$

$$B = \int_{P_s}^0 [D] dp, \quad (4)$$

where the $[P_s]$ denotes the zonal average, and $[D] = \frac{\partial [v]}{\partial y}$ represents the zonally averaged meridional component of convergence. The left hand side of Eq. (2), $(\frac{\partial C}{\partial t})$, represents variation of zonally averaged pressure at both NAM's action centers, while the right side, B , mainly represents the variation of the Ferrel cell. As the total convergence of mass in the troposphere ($\int_{P_s}^{200\text{hPa}} [D] dp$; the 200 hPa isobaric surface is near the tropopause at middle and high latitudes) is much larger than that in the stratosphere ($\int_{200\text{hPa}}^0 [D] dp$), this results in $B \approx \int_{P_s}^{200\text{hPa}} [D] dp$, and $\int_{P_s}^{200\text{hPa}} [D] dp = [w]$ [26, 27], and so $B \approx [w]$, where $[w]$ represents the variation of the Ferrel cell at middle and high latitudes. Therefore, Eq. (2) indicates that the variation of the NAM or surface pressure at middle and high latitudes is mainly determined by the intensity of the Ferrel cell.

Following the method of Cai and Ren [28], the preceding relationship between the temporal evolution of the Ferrel cell and the NAM can be interpreted according to the perturbation solution of Eq. (2), $\frac{\partial C}{\partial t} \approx B$. For a temporal fluctuation of a single harmonic signal (e.g., if $B' = A \cos(lt - np - kt)$, then $C' = [P_s]' \propto \frac{A}{k} \sin(lt - np - kt)$ where $l > 0$, $n > 0$, and $k > 0$), the surface pressure anomalies ($C' = [P_s]'$) should be about a quarter ($\frac{\pi}{2k} = \frac{1}{4} \frac{2\pi}{k}$) period lag behind the total column convergence anomalies ($B' = \int_{P_s}^{200\text{hPa}} [D]' dp + \int_{200\text{hPa}}^0 [D]' dp \approx \int_{P_s}^{200\text{hPa}} [D]' dp$). As the variation of the total convergence of mass in the troposphere ($\int_{P_s}^{200\text{hPa}} [D]' dp$) represents that of the Ferrel cell at middle and high latitudes, the variation of surface pressure (or the NAM) should also lag behind the Ferrel cell by about a quarter ($\frac{\pi}{2k}$) period. Consequently, the lag relationship between the daily variations of the NAM and the Ferrel cell appears reasonable.

The observed lag time of about 1–2 days is also reasonable according to Eq. (2). For a daily NAM event with timescales of around 10 days, the lag of about a quarter period equals the lag of about 2.5 days. Attribute to the tropospheric atmosphere has the shorter variation timescales than the stratospheric and upper atmosphere [29, 30], the preceding time in the troposphere is shorter than that in the stratosphere and upper levels. Specifically, the lead-time (t') of tropospheric convergence anomalies (or Ferrel cell anomalies) is less than a quarter period ($t' < \frac{\pi}{2k}$). For the daily NAM events with timescales of around 10 days, this preceding time of the Ferrel cell or tropospheric convergence anomalies ($[D]'$) to the NAM or surface pressure anomalies ($[P_s]'$) is consequently less than 2.5 days. Therefore, both the lag relationship and the observed lag of 1–2 days between the NAM and Ferrel cell appear to be reasonable.

6 Physical interpretations of the preceding variation of the Ferrel cell in the NAM's phase transition from a mass viewpoint

In the above section, the lag relationship and the number of lag days between the variation of the Ferrel cell and the NAM for daily events were both verified using a pressure tendency equation. The lag relationship between them is difficult to detect over monthly or longer timescales, but is important if we are to increase our understanding of their physical connection process from a mass viewpoint. However, the physical explanation of this lag relationship between the Ferrel cell and the NAM remains to be clarified. To investigate this point, we composited the anomalous FCI, NAMI, P_s , and tropospheric ZMSF (TZMSF) according to the temporal evolution of the daily events of both FCI and NAMI.

The lag relationship and number of lag days between the Ferrel cell and the NAM are captured well by the composited lines of FCI and NAMI in Fig. 5. In the positive FCI or NAM events, the intensity of the Ferrel cell (red lines in Fig. 5a and c) increases prior to the NAM (blue lines in Fig. 5a and c), attains its maximum value 1–2 days before the NAM does, and then drops before the NAM does. Similarly, in the negative Ferrel cell and NAM events (Fig. 5b and d), the variation of the Ferrel cell precedes the NAM. So, the lag relationship between the Ferrel cell and the NAM in the composited maps (Fig. 5) coincides with that in the lead-lag correlation maps (Fig. 3).

We also noticed that the composited TZMSF (color shaded) and P_s (contours) at middle and high latitudes captures the simultaneous variation of mass transport associated with the Ferrel cell and mass redistribution

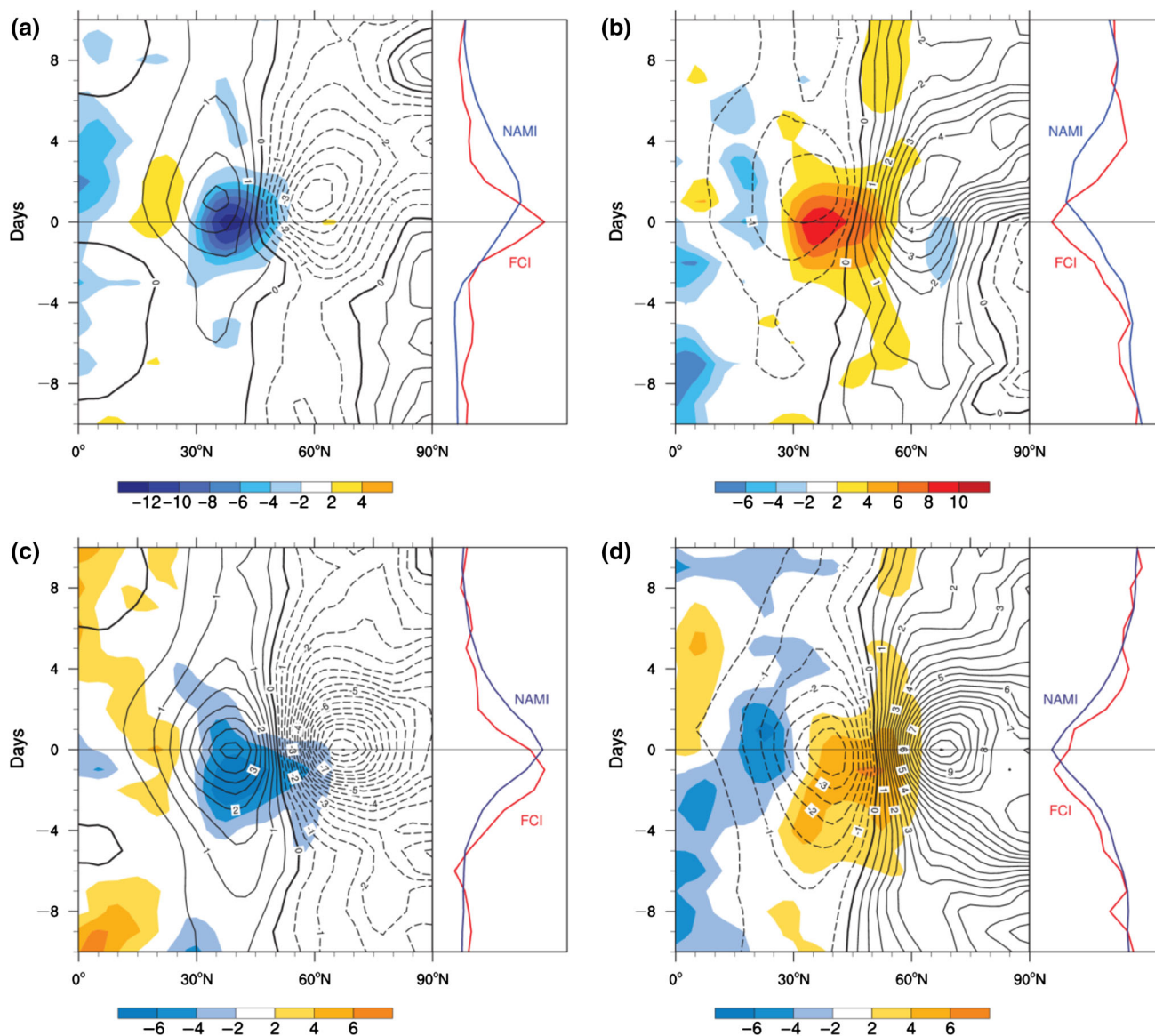


Fig. 5 Composite anomalies (tropospheric net meridional mass flux (10^9 kg s^{-1}): shading; surface pressure (hPa): contours) as a function of latitude (abscissa) and time (ordinate: day), and the accordingly normalized composite FCI (red line) and NAMI (blue line) for: **a** positive FCI events, **b** negative FCI events, **c** positive NAM events, and **d** negative NAM events. A negative value on the ordinate indicates the day before the peak value of the event, and *vice versa*

associated with the NAM very well, as shown in Fig. 5. The TZMSF is the integral of the zonally averaged meridional mass flux from the tropopause (near 200 hPa at middle and high latitudes) downward to the Earth's surface at middle and high latitudes, $\text{TZMSF}(p, \varphi) = \frac{2\pi a \cos(\varphi)}{g} \int_{200 \text{ hPa}}^{P_s} [v(p, \varphi)] dp$; while P_s is the surface pressure and represents the total mass above the surface. As shown in Fig. 5, the TZMSF at middle and high latitudes has a synchronous variation with the FCI (red curves), while the surface pressure (P_s) at middle and high latitudes represents the mass variation in the two action centers of the NAM and both have synchronous variations with NAMI

(blue curves). Therefore, the TZMSF and P_s at middle and high latitudes is a synchronous measurement of the intensity of the Ferrel cell and the NAM, respectively.

As the Ferrel cell and the NAM represents mass transport and mass redistribution, respectively, at middle and high latitudes, we can observe from Fig. 5 that the physical process represented by the lag relationship is the preceding mass transport associated with the Ferrel cell that causes the consequent mass redistribution associated with the phase transition of the NAM. In positive FC and NAM events (Fig. 5a and c), negative TZMSF occurs at middle latitudes around 30° – 60°N , indicating that the atmospheric

mass in the troposphere is transported equatorward from middle and high latitudes to middle and low latitudes by the anomalous Ferrel cell, which causes a subsequent atmospheric mass redistribution 1–2 days later with the mass accumulating in the middle latitudes (ca. 35°N) and dissipating at high latitudes (ca. 65°N). This kind of mass redistribution is represented by an anomalous positive P_s at middle latitudes and a negative P_s at high latitudes; i.e., a positive NAM. Similarly, in negative FC and NAM events (Fig. 5b and d), the processes are reversed, and the anomalously negative Ferrel cell transports the mass from middle and low latitudes back to middle and high latitudes, subsequently resulting in a negative NAM. Therefore, the lag relationship between the Ferrel cell and the NAM is a reflection of the preceding meridional transfer of atmospheric mass back and forth between middle and high latitudes, and this meridional mass transfer causes the subsequent mass redistribution at middle and high latitudes, resulting in the phase transition of the NAM.

This result is well supported by the study of Haynes and Shepherd [31], who demonstrated theoretically that meridional circulations will transport mass and so cause variations in surface pressure. It also indicates that the lag relationship between the Ferrel cell and the NAM has an explicit physical meaning.

7 Discussion and conclusions

In this study, the connections of the NAM with the Ferrel, Hadley, and Polar cells have been re-investigated. We have demonstrated that the Ferrel cell (of the three cells) has the most synchronous seasonal variations with the NAM, and this is in good agreement with previous studies [2, 12]. We attribute this largely to the location of the Ferrel cell, whose ascending and descending branches happen to form a bridge across the NAM's two action centers, or the two so-called annular belts of action in the NH [12]. Further study found that daily variation of the Ferrel cell precedes that of the NAM by 1–2 days. This lag relationship, and the number of lag days, were found to be reasonable and were verified using the surface pressure tendency equation. This lead-lag relationship is difficult to detect on monthly or longer timescales, but is important if we are to improve our knowledge of the mass transport processes and physical connections between the NAM and general circulations, especially the role played by the Ferrel cell in daily variability of the NAM. Through the compositing of the temporary evolution of mass flux and surface pressure under the context of the daily fluctuations of the NAM and the Ferrel cell, we revealed that this statistically identified temporal phase difference between NAM and Ferrel cell variability can be elucidated by meridional mass redistribution. The

preceding variation of the Ferrel cell indicates the leading meridional mass transport between middle and high latitudes, which causes changes in mass redistribution between middle and high latitudes, and results in the phase transition of the NAM 1–2 days later. Therefore, the lag relationship between the NAM and the Ferrel cell has a physical meaning and it indicates the preceding mass transport associated with the anomalous Ferrel cell causes the consequent phase mass redistribution associated with the transition of the NAM.

This study focused on daily timescales from the viewpoint of meridional mass transport and conservation, which is helpful in extending our understanding of the connections between the NAM and Ferrel cell variability. Our study also supports previous findings related to the connection between the NAM and the Ferrel cell. For example, Xiao et al. [32] found that the decadal variation of the NAM in the mid-1980s was accompanied by that of the Ferrel cell and that of the meridional mass exchange between middle and high latitudes. Their conclusions are supported by the existence of the lag relationship (demonstrated here) between the Ferrel cell and the NAM over short timescales. Thus, the results of this study place the related previous work in a more rounded context.

The NAM is difficult to be predicted because of the low predict probability of the atmospheric process in middle and high latitudes [33–37]. After the stratospheric signals are seen as an efficient predictor of NAM [29, 38–40], the prediction of the NAM variability attracts more and more considerable attention. The lag relationship documented in this study implies that the intensity of Ferrel cell may act as another new predictor for the NAM and local weather systems. Therefore, the results in this study may help to improve the operational prediction systems of the NAM and local weather. One question also arises: what is the skill of the Ferrel cell in short-weather and extended-range weather forecasts? Further work will be required to answer this question.

Acknowledgments We thank Dr. Jie Song and two anonymous reviewers for their valuable comments. This work was supported by the National Natural Science Foundation of China (40905040 and 41030961), the National Basic Research Program of China (2010CB950400), and the R&D Special Fund for Public Welfare Industry of China (meteorology) (GYHY201306031).

Conflict of Interest The authors declare that they have no conflict of interest.

References

1. Thompson DWJ, Wallace JM (1998) The Arctic Oscillation signature in the wintertime geo potential height and temperature fields. *Geophys Res Lett* 25:1297–1300

2. Thompson DWJ, Wallace JM (2000) Annular modes in the extratropical circulation. Part 1: month-to-month variability. *J Clim* 13:1000–1016
3. Yamazaki K, Shinya Y (1999) Analysis of the Arctic Oscillation simulated by AGCM. *J Meteorol Soc Jpn* 77:1287–1298
4. Limpasuvan V, Hartmann DL (2000) Wave-maintained annular modes of climate variability. *J Clim* 13:4414–4429
5. Wu Z, Wang B, Li J et al (2009) An empirical seasonal prediction model of the East Asian summer monsoon using ENSO and NAO. *J Geophys Res* 114:D18120. doi:10.1029/2009JD011733
6. Li J, Yu R, Zhou T (2008) Teleconnection between NAO and climate downstream of the Tibetan Plateau. *J Clim* 21:4680–4690
7. McAfee SA, Russell JL (2008) Northern Annular Mode impact on spring climate in the western United States. *Geophys Res Lett* 35:L17701. doi:10.1029/2008GL034828
8. Li Y, Lu H, Jarvis MJ et al (2011) Nonlinear and nonstationary influences of geomagnetic activity on the winter North Atlantic Oscillation. *J Geophys Res* 116:D16109. doi:10.1029/2011JD015822
9. Dickson R, Osborn T, Hurrell J et al (2000) The arctic ocean response to the North Atlantic Oscillation. *J Clim* 13:2671–2696
10. Rigor IG, Wallace JM, Colony RL (2002) Response of sea ice to the Arctic Oscillation. *J Clim* 15:2648–2663
11. de Beurs KM, Henebry GM (2008) Northern Annular Mode effects on the land surface phenologies of Northern Eurasia. *J Clim* 21:4257–4279
12. Li J, Wang JXL (2003) A modified zonal index and its physical sense. *Geophys Res Lett* 30:1632. doi:10.1029/2003GL017441
13. Feldstein SB (2000) The timescale, power spectra, and climate noise properties of tele connection patterns. *J Clim* 13:4430–4440
14. Feldstein SB (2002) The recent trend and variance increase of the annular mode. *J Clim* 15:88–94
15. Feldstein SB (2003) The dynamics of nao tele connection pattern growth and decay. *Quart J Roy Meteorol Soc* 129:901–924
16. Thompson DWJ, Lee S, Baldwin MP (2003) Atmospheric processes governing the Northern Hemisphere Annular Mode/North Atlantic Oscillation. In: Hurrell JW, Kushnir Y, Visbeck M et al (eds) *The North Atlantic Oscillation: climatic significance and environmental impact*. American Geophysical Union, Washington DC, pp 81–112
17. Robinson WA (2000) A baroclinic mechanism for the eddy feedback on the Zonal Index. *J Atmos Sci* 57:415–422
18. Kalnay E, Kanamitsu M, Kistler R et al (1996) The NCEP/NCAR 40-year reanalysis project. *Bull Am Meteorol Soc* 77:437–471
19. Li X, Li J (2009) Main sub monthly timescales of Northern and Southern Hemisphere Annual Modes. *Chin J Atmos Sci* 33:215–231 (in Chinese)
20. Li X, Li J, Zhang X (2013) A two-way stratosphere-troposphere coupling of sub monthly zonal-mean circulations in the arctic. *Adv Atmos Sci* 30:1771–1785
21. Oort AH, Yienger JJ (1996) Observed interannual variability in the Hadley Circulation and its connection to ENSO. *J Clim* 9:2751–2767
22. Peixoto JP, Oort AH (1992) *Physics of climate*. American Institute of Physics, New York, p 520
23. Waliser DE, Shi Z, Lanzante JR et al (1999) The Hadley Circulation: assessing NCEP/NCAR reanalysis and sparse *in-situ* estimates. *Climate Dyn* 15:719–735
24. Benedict JJ, Lee S, Feldstein SB (2004) Synoptic view of the North Atlantic Oscillation. *J Atmos Sci* 61:121–144
25. Baldwin MP (2001) Annular modes in global daily surface pressure. *Geophys Res Lett* 28:4115–4118
26. Holton JR (2004) Surface pressure tendency. In: Cynar F, Hele J (eds) *An introduction to dynamic meteorology*. Elsevier, San Diego, pp 77–79
27. Li X, Li J (2012) Analysis of the quasi-geostrophic adjustment process of the Southern Hemisphere Annular Mode. *Chin J Atmos Sci* 36:755–768 (in Chinese)
28. Cai M, Ren RC (2006) 40–70 day meridional propagation of global circulation anomalies. *Geophys Res Lett* 33:L06818
29. Baldwin MP, Stephenson DB, Thompson DWJ et al (2003) Stratospheric memory and skill of extended-range weather forecasts. *Science* 301:636–640
30. Cai M, Ren RC (2007) Meridional and downward propagation of atmospheric circulation anomalies. Part I: Northern hemisphere cold season variability. *J Atmos Sci* 64:1880–1901
31. Haynes P, Shepherd T (1989) The importance of surface pressure changes in the response of the atmosphere to zonally-symmetric thermal and mechanical forcing. *Q J R Meteorol Soc* 115:1181–1208
32. Xiao D, Li J, Zhao P (2012) Four-dimensional structures and physical process of the decadal abrupt changes of the northern extratropical ocean-atmosphere system in the 1980s. *Int J Climatol* 32:983–994
33. Davis RE (1976) Predictability of sea surface temperature and sea level pressure anomalies over the north pacific ocean. *J Phys Oceanogr* 6:249–266
34. Reichler T, Roads JO (2004) Time-space distribution of long-range atmospheric predictability. *J Atmos Sci* 61:250–263
35. Bengtsson L, Hodges KI, Froude SRL (2005) Global observations and forecast skill. *Tellus A* 57:515–527
36. Li J, Ding R (2011) Temporal-spatial distribution of atmospheric predictability limit by local dynamical analogs. *Mon Weather Rev* 139:3265–3283
37. Li J, Ding R (2013) Temporal-spatial distribution of the predictability limit of monthly sea surface temperature in the global oceans. *Int J Climatol* 33:1936–1947
38. Baldwin MP, Dunkerton TJ (1999) Propagation of the arctic oscillation from the stratosphere to the troposphere. *J Geophys Res* 104:30937–30946
39. Baldwin MP, Dunkerton TJ (2001) Stratospheric harbingers of anomalous weather regimes. *Science* 294:581–584
40. Baldwin MP, Thompson DWJ, Shuckburgh EF et al (2003) Weather from the stratosphere? *Science* 301:317–319